

Received September 19, 2019, accepted October 9, 2019, date of publication October 14, 2019, date of current version October 25, 2019.

Digital Object Identifier 10.1109/ACCESS.2019.2947346

Simplified Estimation of Junction Temperature Fluctuation at the Fundamental Frequency for IGBT Modules Considering Mission Profile

XIPING WANG^{ID}, ZHIGANG LI, FANG YAO, AND SHENGXUE TANG

State Key Laboratory of Reliability and Intelligence of Electrical Equipment, School of Electrical Engineering, Hebei University of Technology, Tianjin 300130, China

Key Laboratory of Electromagnetic Field and Electrical Apparatus Reliability of Hebei Province, School of Electrical Engineering, Hebei University of Technology, Tianjin 300130, China

Corresponding author: Xiping Wang (ndwangxiping@163.com)

This work was supported in part by the National Natural Science Foundation of China under Grant 51377044, and in part by the Key Project of Hebei Province Natural Science Foundation under Grant E2017202284.

ABSTRACT The junction temperature at the fundamental frequency cannot be ignored in a lifetime evaluation of insulated-gate bipolar transistors (IGBTs) with a long-term mission profile. Therefore, it is very important in terms of calculation speed and accuracy to simplify the loss curve when calculating the thermal fluctuation at the fundamental frequency. This paper proposes a mathematical analysis method for the junction temperature fluctuation at the fundamental frequency based on an equivalent sinusoidal half-wave loss. The dynamic and static parameters of the devices are tested by an experimental platform, and accurate device loss models are established through a case study of a 1.5 MW direct-drive wind turbine grid-connected model. The accuracy of the proposed calculation model is compared with that of a time-domain simulation and the two-step loss pulse method. Considering different output frequencies, the accuracy of the proposed method is further discussed. Based on actual wind speed data, the proposed method is used to calculate the junction temperature of an IGBT module in a grid-side converter. The results show that the proposed method can improve the accuracy of the reliability evaluation of wind power converters.

INDEX TERMS Junction temperature fluctuation, equivalent sinusoidal half-wave loss, fundamental frequency, reliability, mission profile.

I. INTRODUCTION

In recent years, wind energy has developed rapidly as a clean renewable energy source, and the capacity of wind turbines has increased continuously. Especially for the large-scale grid-connected transmission of wind power generation, large-capacity and high-reliability requirements are receiving more and more attention [1]–[3]. The wind power converter is the key component of wind turbines. The wind power converter plays an important role in the flexible operation of units and in the safe and stable operation of the power grid. Limited by wind resources, wind power converters are often in a remote and harsh operating environment, especially offshore wind turbines, which is one of the most vulnerable parts of wind power plants. Therefore, improving the reliability of the con-

verter can ensure the safe operation of the generator set. More importantly, a long converter life is the main factor to consider for reducing the cost of wind power generation [4]–[6].

The reliability of a wind power converter system is affected not only by the circuit topology but also by the reliability of the devices, which plays a decisive role in the system [7], [8]. The IGBT module is the most valuable key device inside the converter. In [7], the six IGBT modules of the inverter system are in series, and any failure (ignoring a redundant design) will result in a failure of the converter system. Operating under the coupled action of electrothermomechanical fields, IGBT modules are required to have a high reliability to improve the system reliability. Based on the principle of barrel theory, the reliability of a power module depends on the lifetime of the internal weak link (IGBT or diode) [9]. In the literature [10], [11], an in-depth analysis of the IGBT module failure mechanism pointed out that the IGBT module package

The associate editor coordinating the review of this manuscript and approving it for publication was Kalyan Koley^{ID}.

has a multilayer structure inside the module, in which the thermal expansion coefficients of the layers are mismatched. The structure of each layer of the module needs to withstand a considerable heat expansion and contraction process. Thermal stress and long-term repeated temperature fluctuations are the main factors affecting the working life of IGBT modules. An accurate power loss and junction temperature fluctuation analysis is important for the reliability analysis and thermal design of high-power IGBT modules [12]. For every 10°C increase in temperature, the failure rate of the switching device doubles [13]. A transient high temperature is an important cause of an external failure of the device, so the junction temperature information is the basis for device life prediction and management [14]. Under the operating conditions of an actual power electronic system, it is difficult to directly obtain the power loss and junction temperature of the device. Therefore, it is necessary to estimate the thermal load of the wind power converter according to the mission profile. The lifetime prediction of the IGBT module usually takes into account the wind speed and air temperature in the wind power converter over a long time (one year), spanning multiple time scales. Therefore, converting the operating conditions into thermal loading is key for a lifetime consumption assessment of the components [15], [16]. The accuracy of a lifetime cumulative damage assessment is limited by the accuracy of the junction temperature calculation of the power device.

In addition to the wind speed, temperature, and other external environmental factors, the junction temperature fluctuation at the fundamental frequency cannot be ignored in a lifetime assessment. The fundamental wave of the grid-side converter output current maintains the same frequency as the grid voltage ($f_0 = 50$ Hz), and the junction temperature calculation needs to process approximately 1.57×10^9 power cycles in one year. Therefore, it is very important to be able to obtain the thermal load that meets the calculation accuracy requirements within a reasonable calculation time.

The electrothermal coupling iteration based on a time-domain simulation is a very accurate method for calculating the junction temperature, but the method has a very long simulation time. For long-term mission profiles, large amounts of data are generated during the calculation. It is unrealistic to apply this method to the reliability research of power modules. Based on the electrothermal analogy method, studies [17] and [18] have specified the iterative principle and calculation process of the junction temperature for IGBT modules in wind power converters, which uses the Gauss-Seidel junction temperature iteration to calculate the junction temperature at the fundamental frequency. The calculation results show that the method is fast and accurate, but the method cannot be used in systems with nonconvergence. The finite element numerical calculation method is accurate when based on a three-dimensional physical model and can reflect the three-dimensional distribution characteristics of the steady-state and transient junction temperatures. However, the physical modeling of IGBT modules is complex and the amount of computation is large, which is not suitable for

calculating the junction temperature of devices over a long time [19]. For high-power IGBT modules, the power loss has sinusoidal half-wave characteristics [20]. Therefore, some scholars have proposed a simplified loss model to improve the speed of calculating the junction temperature fluctuation but at the expense of the calculation accuracy. Reference [21] proposed a calculation method for a two-step loss pulse sequence, which can quickly calculate the junction temperature fluctuation and the average junction temperature of devices. The transition process of the instantaneous junction temperature is neglected in order to improve the calculation speed. Thus, there is a certain error in the junction temperature of the device calculated by this method. Reference [22] considered the inherent DC bias characteristics of a modular multilevel converter (MMC) and proposed a mathematical iterative method based on a virtual sinusoidal half-wave loss approximation to calculate the junction temperature fluctuation of power devices in the MMC, and the validity of the method was verified.

In this paper, the impulse equalization principle is introduced into the junction temperature calculation of a wind power converter, and a calculation method for the junction temperature fluctuation is proposed that is suitable for a long-term mission profile reliability evaluation of wind power converters. First, the average junction temperature iterative calculation method is analyzed based on electrothermal coupling at the fundamental frequency. Then, the average loss is equivalent to sinusoidal half-wave loss, and the mathematical analytical model is derived for a fast calculation of the steady-state junction temperature fluctuation. In a 1.5 MW grid-connected direct-drive wind generator case study, the dynamic and static parameters are tested through experiments to establish the device loss models. The accuracy of the proposed model is compared with a time-domain electrothermal simulation and the two-step loss method. The impacts of different output frequencies on the junction temperature fluctuation calculations are further discussed and compared with those of other calculation methods. Finally, based on actual wind speed data, the junction temperature of the IGBT module is calculated by the proposed method, and the effectiveness of the proposed method is verified.

II. JUNCTION TEMPERATURE CALCULATION MODEL BASED ON AN EQUIVALENT SINUSOIDAL HALF-WAVE LOSS

A. PROCESS OF THE PROPOSED METHOD

Fig. 1 illustrates the calculation process of the average junction temperature and the thermal fluctuation estimation of the power device in a wind power converter. Before the junction temperature evaluation process, the measured wind speed data needs to be converted into the converter output power according to the wind farm wind power curve. The operating parameters of the converter are the voltage modulation coefficients, the DC bus voltage, the device current, output frequency, and other electrical parameters. In the flow

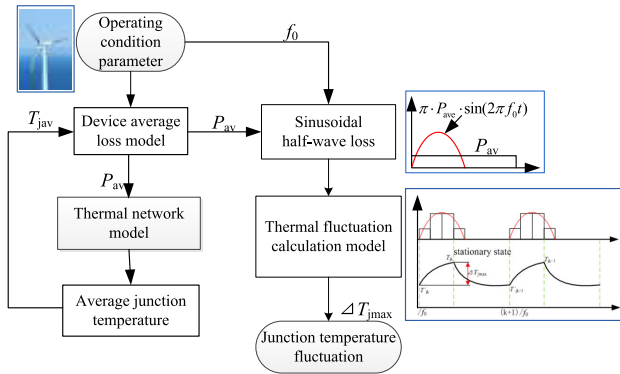


FIGURE 1. Flowchart of the proposed method.

chart, the operation parameters of the wind power are input into the average loss model based on the power frequency f_0 . Then the electrothermal coupling iterative calculation is conducted to obtain the average junction temperature $T_{j\text{av}}$ and average loss P_{av} . The process above iterates until the junction temperature $T_{j\text{av}}$ converges. The average loss is converted into a sinusoidal half-wave loss. According to the principle of area equivalence, the equivalent rectangular pulse loss of the sinusoidal half-wave loss into the calculation model of the steady-state junction temperature fluctuation, the maximum fluctuation value $\Delta T_{j\text{max}}$ can be obtained. This method is applicable to the junction temperature calculation for the grid side and the machine side in the converter.

B. ITERATIVE CALCULATION OF THE AVERAGE LOSS CONSIDERING JUNCTION TEMPERATURE COUPLING

The average losses of the IGBT and diode include the average conduction losses P_{cond} of the devices and the average switching losses P_{sw} (or reverse recovery losses) at the output power frequency. The output characteristics and switching losses of the devices can be obtained through experiments or a datasheet. Taking the grid-side inverter as an example, the junction temperature of the chip is evaluated and iteratively calculated when calculating the average conduction losses of the IGBT and the diode to better consider the electrothermal interaction characteristics under operating conditions. The average conduction loss of the power device is expressed as

$$P_{\text{cond}} = f_0 \int_0^{1/(2f_0)} U_{\text{ce}}(t) \cdot i(t) \cdot \delta(t) dt \quad (1)$$

where $\delta(t)$ represents the switching duty cycle of the power device, U_{ce} represents the forward on-state voltage drop of the power device, and i represents the current flowing through the power device. The calculation of the above integral formula is more complicated. According to (1), the numerical calculation can be expressed as [23]

$$P_{\text{cond}} = \sqrt{2}I_c \cdot \left(\frac{1}{2\pi} \pm \frac{m \cdot \cos \varphi}{8}\right) \cdot V_0(T_j) + 2 \cdot I_c^2 \left(\frac{1}{8} \pm \frac{m \cdot \cos \varphi}{3\pi}\right) \cdot r(T_j) \quad (2)$$

in which the positive sign indicates the IGBT calculation formula, and the negative sign indicates the diode calculation formula. m represents the voltage modulation factor, $\cos \varphi$ represents the power factor, I_c represents the output current RMS of the grid side, and T_j represents the junction temperature of the device. V_0 represents the threshold voltage at the corresponding junction temperature, r represents the on-resistance at the corresponding junction temperature, and the output characteristic curve of the IGBT can be used with the junction temperatures $T_1 = 25^\circ\text{C}$ and $T_2 = 125^\circ\text{C}$. The two parameters at the corresponding junction temperature are calculated by approximating the interpolation by the following formulas.

$$V_0(T_j) = \frac{V_0(T_2) - V_0(T_1)}{T_2 - T_1} (T_j - T_1) + V_0(T_1) \quad (3)$$

$$r(T_j) = \frac{r(T_2) - r(T_1)}{T_2 - T_1} (T_j - T_1) + r(T_1) \quad (4)$$

The switching losses (reverse recovery losses) of the IGBTs and diodes are related to the conduction current, junction temperature, DC voltage, and drive resistance and can be obtained as [24]

$$P_{\text{sw}(T)} = f_{\text{sw}} \cdot E_{\text{on+off}} \cdot \frac{1}{\pi} \cdot \frac{\sqrt{2}I_c}{I_{\text{ref}}} \cdot \left(\frac{V_{\text{DC}}}{V_{\text{ref}}}\right)^{K_V} \cdot (1 + C_T(T_j - T_{\text{ref}})) \quad (5)$$

$$P_{\text{sw}(D)} = f_{\text{sw}} \cdot E_{\text{rr}} \cdot \frac{1}{\pi} \cdot \frac{\sqrt{2}I_c}{I_{\text{ref}}} \cdot \left(\frac{V_{\text{DC}}}{V_{\text{ref}}}\right)^{K_V} \cdot (1 + C_T(T_j - T_{\text{ref}})) \quad (6)$$

where E_{on} and E_{off} represent the turn-on and turn-off energy consumptions under IGBT rated conditions, V_{DC} represents the DC-side voltage, K_V and C_T can be calculated by an experiment or a datasheet. i_{ref} , V_{ref} , and T_{ref} represent the reference current, reference blocking voltage, and reference temperature, respectively. f_{sw} represents the switching frequency. Under the same load current, the higher the switching frequency is, the better the quality of the output voltage waveform. However, the switching losses are directly proportional to f_{sw} [25]. f_{sw} is limited by the maximum junction temperature and the efficiency of the converter.

It is known from the electrothermal analogy method that the thermal model of the device can be represented by an equivalent circuit. To meet the accuracy requirements of the thermal model, a fourth-order Foster thermal network is generally established for the IGBT module. To speed up the calculation of the average junction temperature iterative calculation, the network uses a pure thermal resistance network model ignoring the average junction temperature transient process. As shown in Fig. 2, the temperature is represented by the node voltage. $T_{j,T} / T_{j,D}$, and $T_{c,T} / T_{c,D}$ represent the junction temperature and case temperature of the IGBT/diode chip, respectively. The IGBT module contains two heat sources, the IGBT and the diode chip, which are represented by P_T and P_D , respectively. R_{tjci} , R_{dici} ($i = 1, 2, 3, 4$) is the thermal resistance of the IGBT/diode chip

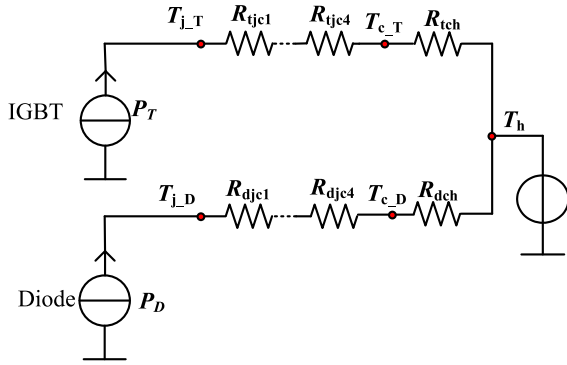


FIGURE 2. Thermal model for the IGBT modules.

relative to the resistance of the case, R_{tch}/R_{dch} is the thermal resistance of the IGBT/diode case relative to the resistance of the heat sink, and T_h is the heat sink temperature. Here, the heat sink time is constant at the level of minutes. When calculating the junction temperature fluctuation at the fundamental frequency, the temperature increase of the heat sink is not considered [26]. Based on the feedback of the junction temperature, the average periodic loss at the fundamental frequency is input into the thermal network model for the iterative calculation. Then, the average junction temperature and average loss of the power devices are obtained under the corresponding working conditions.

C. CALCULATION MODEL OF THE THERMAL FLUCTUATION AT THE FUNDAMENTAL FREQUENCY

First, the average loss of the IGBT (diode) needs to be converted into an equivalent half-wave loss using (7). As shown in Fig. 3, the sinusoidal half-wave loss is divided into 4 dissipation pulses for the thermal estimation while the negative half cycle loss is zero. As shown in Fig. 5, because the minimum time of the thermal response is 1 ms, the maximum number of pulse losses is 10 for a 50 Hz fundamental frequency output, but the calculation is very time-consuming. Therefore, 4 dissipation pulses are used here. Then, four equivalent pulse losses $P_i (i=1,2,3,4)$ are obtained with reference to (8) according to the principle of equal impulse area. In addition, $P_1 = P_4, P_2 = P_3$, as shown in (9) and (10).

$$P_{peak(T/D)} = \pi \cdot P_{ave(T/D)} = \pi \cdot (P_{con} + P_{sw(T/D)}) \quad (7)$$

$$P_i = \frac{1}{\Delta t} \int_{i-1/\Delta t}^{i/\Delta t} \pi \cdot P_{ave} \sin(2\pi f_0 \cdot t) dt \quad (8)$$

$$P_1 = P_4 = 2(2-\sqrt{2}) \cdot P_{ave} \quad (9)$$

$$P_2 = P_3 = 2\sqrt{2} \cdot P_{ave} \quad (10)$$

where $\Delta t = 1/(8 \cdot f_0)$.

To convert the power loss based on the power frequency into the thermal load, the equivalent rectangular pulse loss is input into the thermal impedance model of the power device. Then, the value of the maximum junction temperature fluctuation ΔT_j is obtained at the fundamental frequency. The fluctuation of the junction temperature in the thermal loading

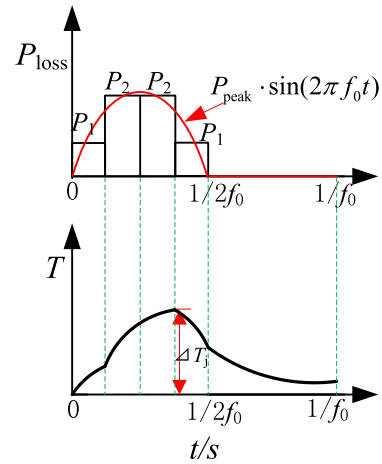


FIGURE 3. Calculation of the junction temperature fluctuation based on an equivalent sinusoidal half-wave loss.

is mainly caused by the fast and periodic alternation of the load current [16]. However, in the initial stage, the junction temperature of the device is transient. The two-step pulse loss method based on the simplified loss model ignores the transient junction temperature transition process [21]. In addition, the first junction temperature fluctuation is considered to be the steady-state junction temperature fluctuation, which will result in inaccuracies when predicting the junction temperature.

Actually, Fig. 4 illustrates the simplification of the equivalent rectangular power loss and its thermal response process. After several fundamental periods, the junction temperature reaches a steady state. The average junction temperature no longer increases, and the final junction temperature fluctuates around the average of the average junction temperature. At this moment, the power loss and dissipated power reach a balance. The maximum value of fluctuation ΔT_{jmax} in steady state is the amplitude of the fluctuation in the fundamental frequency cycle. For a more accurate prediction with the minimum number of computations, the derivation process is as follows

$$\begin{cases} T'_{j0} = 0 \\ T_{j0} = P_1 \cdot R(1 - \exp(-3\Delta t/\tau)) + (P_2 - P_1) \\ \quad \cdot R(1 - \exp(-2\Delta t/\tau)) \\ T'_{j1} = T_{j0} \cdot \exp(-5\Delta t/\tau) + P_1 \cdot R(1 - \exp(-\Delta t/\tau)) \\ \quad \cdot \exp(-4\Delta t/\tau) \\ T_{j1} = T'_{j1} \\ \quad \cdot \exp(-3\Delta t/\tau) + T_{j0} \\ \dots \\ T'_{jk+1} = T_{jk} \cdot \exp(-5\Delta t/\tau) + P_1 \cdot R(1 - \exp(-\Delta t/\tau)) \\ \quad \cdot \exp(-4\Delta t/\tau) \\ T_{jk+1} = T'_{jk+1} \cdot \exp(-3\Delta t/\tau) + T_{j0} \end{cases} \quad (11)$$

According to Fig. 4, when the junction temperature transitions to steady state, the two steady-state junction temperature peaks are equal; namely, $T_{jk+1} = T_{jk}$. Substituting T'_{jk+1}

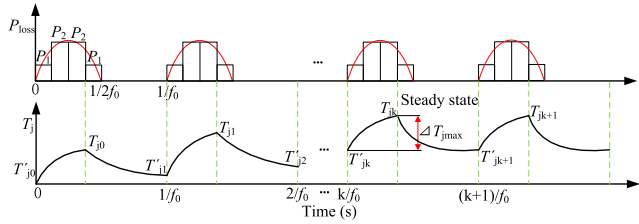


FIGURE 4. Schematic diagram of the junction temperature transition from the transient stage to the steady-state stage.

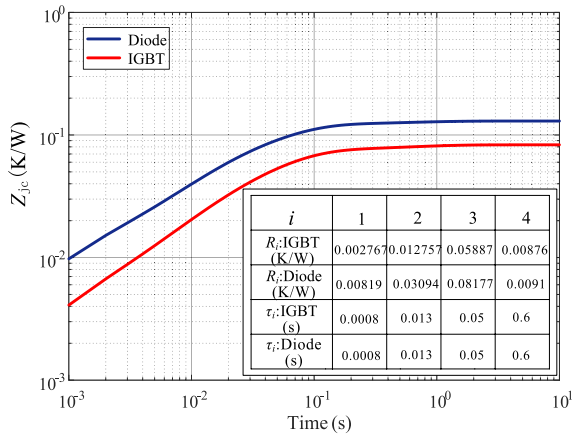


FIGURE 5. Transient thermal impedance curve.

into the thermal estimation equation T_{jk+1} in (11), T'_{jk+1} is eliminated. T_{jk} is expressed as

$$T_{jk} = \frac{P_1 \cdot R(1 - \exp(-\Delta t/\tau)) \cdot \exp(-7\Delta t/\tau) + T_{j0}}{1 - \exp(-8\Delta t/\tau)} \quad (12)$$

Similarly, the minimum junction temperature T'_{jk} can be obtained, which can be expressed as

$$T'_{jk} = \frac{P_1 \cdot R(1 - \exp(-\Delta t/\tau)) \cdot \exp(v - 4\Delta t/\tau) + T_{j0} \exp(-5\Delta t/\tau)}{1 - \exp(-8\Delta t/\tau)} \quad (13)$$

Therefore, the value of the junction temperature fluctuation ΔT_{jmax} at steady state can be obtained, which is given as (14), shown at the bottom of the next page.

To estimate the junction temperature accurately, the high-order thermal impedance curve in the datasheet is adopted, instead of the simplified first-order thermal network. The fourth-order foster thermal impedance (Z_{jc}) curve of the IGBT module is shown in Fig. 5. There are four corresponding thermal time constants τ and four thermal resistance constants R . Substituting T_{j0} into the junction temperature fluctuation (14), the above formula can be expressed as (15), shown at the bottom of the next page.

According to (15), the fluctuation of the junction temperature in the power frequency period can be calculated. The waveform of the change in the junction temperature in the whole period cannot be obtained by the proposed method. This is the focus of this study. The proposed method solves the temperature fluctuation of the fundamental frequency output

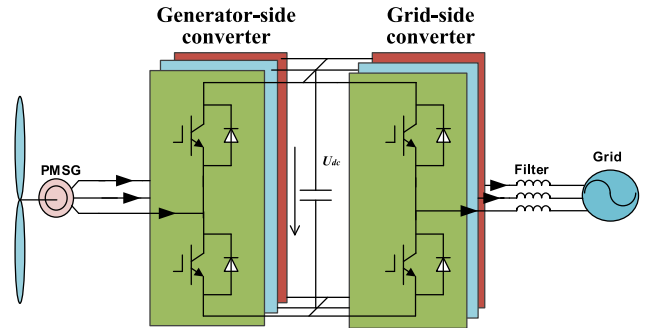


FIGURE 6. Typical structure of a back-to-back direct-drive wind turbine, where the grid-side converter is studied.

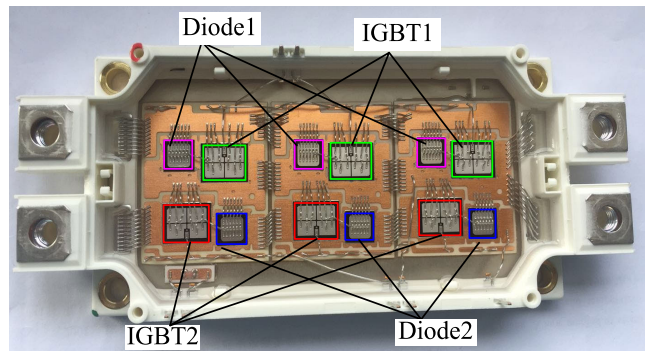


FIGURE 7. Internal structure of unpacked FF300R17ME4 module.

TABLE 1. Specifications of the grid-side converter.

Parameter	Value
Rated active power P_0	1.5 MW
Output power factor $\cos\phi$	1
DC bus voltage V_{dc}	900 V
Grid-side line voltage V_L	480 V
Fundamental frequency f_0	50 Hz
Switching frequency f_{sw}	2 kHz
Filter inductance L	1.2 mH
IGBT module	Infineon FF300R17ME4

cycle (usually one year) quickly and effectively, which is helpful for the evaluation of the reliability of power devices.

III. VALIDATION OF THE PROPOSED METHOD

In this part, the grid-connected inverters of direct-drive wind turbines are taken as an example to analyze the accuracy of this method. A simulation model of a 1.5 MW grid-side inverter is developed in the MATLAB and PLECS cosimulation platform, as shown in Fig. 6. Assuming that all of the power of the machine-side converter is transmitted to the grid-side inverters, the specifications are listed in Table 1. The DC bus voltage is 900 V, and the grid-side line voltage is 480 V. In this study, we employ the Infineon half-bridge module FF300R17ME4, which consists of 6 IGBT chips and 6 antiparallel diode chips. In more detail, the considered IGBT module contains three half-bridge converters connected in parallel, as shown in Fig. 7. For the power modules, the rating of 1.7 kV and 0.3 kA is adopted for the

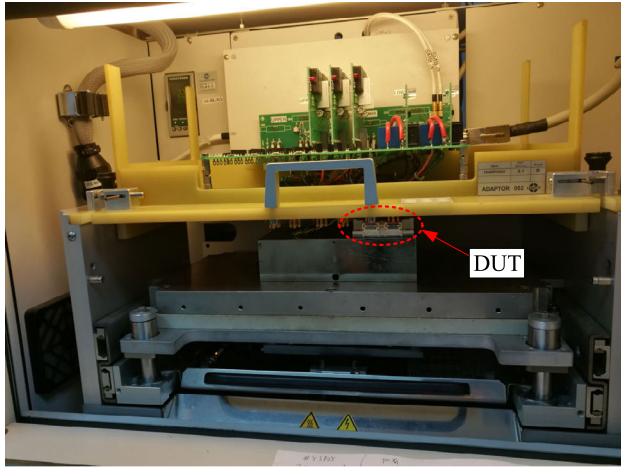


FIGURE 8. Test platform for the IGBT dynamic and static parameters.

grid-side inverter. The multimodule parallel connection meets the capacity requirements of the wind turbine, and the thermal impedance curve of the selected module is shown in Fig. 5.

A. DYNAMIC AND STATIC PARAMETER TESTING

The datasheets of power devices mostly only provide only dynamic and static parameters at 25°C and 125°C. In addition, the switching loss and conduction loss cannot be obtained at other junction temperatures. To calculate the conduction loss and switching loss more accurately, the LEMSYS high-power IGBT tester is used to test the dynamic and static parameters of the device at different temperatures (25°C, 50°C, 75°C, 100°C, and 125°C). The test platform is shown in Fig. 8. The same IGBT module as that in the simulation model is chosen in the experiment.

The static parameters reflect the forward output characteristics of the IGBT and diode at different junction temperatures. The test results are shown in Fig. 9. With the increase in temperature, the forward voltage of the IGBT and diode increases continuously, which means that the conduction

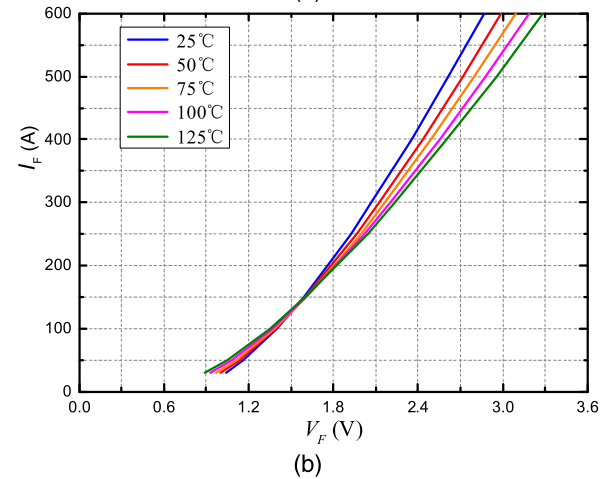
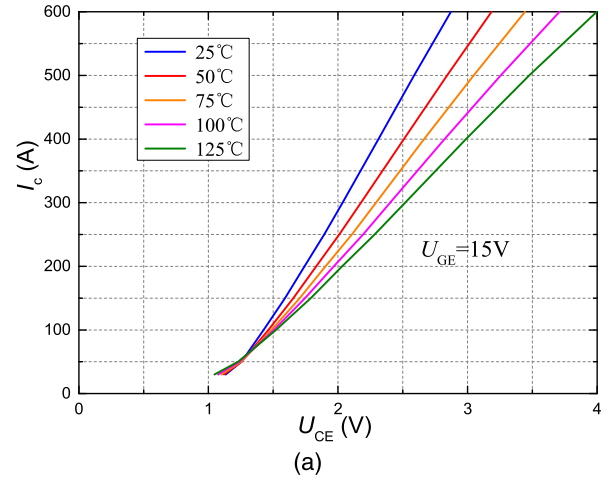


FIGURE 9. Output characteristic of the IGBT and the forward characteristic of the diode at different temperatures. (a) IGBT. (b) Diode.

losses increase continuously. In the dynamic parameter test, the blocking voltage is set to 900 V. The module is heated to a specified temperature by a heating plate using a double-pulse circuit [27]. The switching losses of the IGBT and diode at different temperatures are tested. The test results are shown

$$\begin{cases} \Delta T_{j\max} = T_{jk} - T'_{jk} \\ \Delta T_{j\max} = \frac{P_1 \cdot R(1 - \exp(-\Delta t/\tau)) \cdot (\exp(-7\Delta t/\tau) - \exp(-4\Delta t/\tau)) + T_{j0} \cdot (1 - \exp(-5\Delta t/\tau))}{1 - \exp(-8\Delta t/\tau)} \end{cases} \quad (14)$$

$$\begin{aligned} \Delta T_{j\max} &= P_1 \sum_{i=1}^4 \frac{R_i(1 - \exp(-\Delta t/\tau_i)) \cdot (\exp(-7\Delta t/\tau_i) - \exp(-4\Delta t/\tau_i))}{1 - \exp(-8\Delta t/\tau_i)} \\ &+ P_1 \sum_{i=1}^4 \frac{R_i(1 - \exp(-\Delta t/\tau_i)) \cdot (1 - \exp(-5\Delta t/\tau_i))}{1 - \exp(-8\Delta t/\tau_i)} \\ &+ (P_2 - P_1) \sum_{i=1}^4 \frac{R_i(1 - \exp(-2\Delta t/\tau_i)) \cdot (1 - \exp(-5\Delta t/\tau_i))}{1 - \exp(-8\Delta t/\tau_i)} \end{aligned} \quad (15)$$

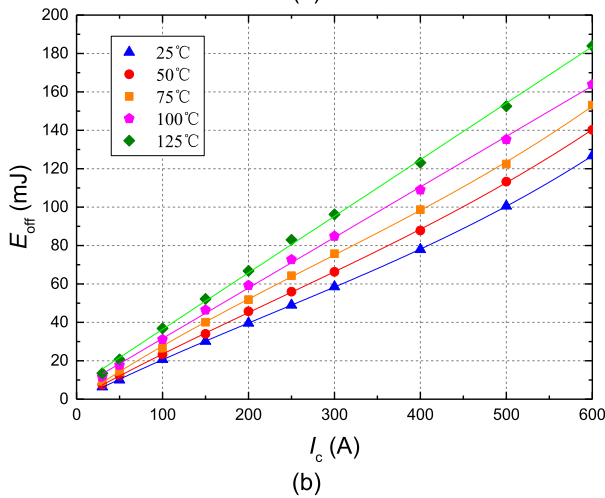
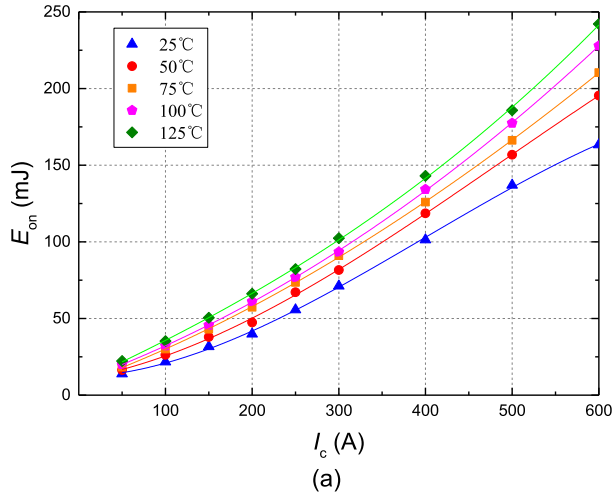


FIGURE 10. Switching losses of the IGBT. (a) Turn-on loss E_{on} . (b) Turn-off loss E_{off} .

in Figs. 10 and 11. The turn-on and turn-off losses of the IGBT increase when the temperature increases. The recovery losses of the diode increase when the temperature increases.

B. VERIFICATION OF THE ACCURACY OF THE THERMAL FLUCTUATION MODEL

To speed up the calculation in PLECS, a lookup table is used to determine the device losses [28], [29]. In a real system, device losses depend on the junction temperature. Based on the above experimental results, the dynamic and static parameters are inputted to the device model in the form of a thermal description file, and an accurate loss model can be obtained. Fig. 12 shows the thermal simulation results of the power devices when the power output current of the grid-side wind power converter is 230 A. The maximum junction temperature of the IGBT chip is approximately 76.8°C, and the fluctuation of the junction temperature $\Delta T_{j/T}$ is approximately 10.3°C. The maximum junction temperature of the diode chip is approximately 56.3°C, and the fluctuation of the junction temperature $\Delta T_{j/D}$ is approximately 4.9°C. The simulation results are used as a benchmark. Based on the same average loss, the proposed calculation method for

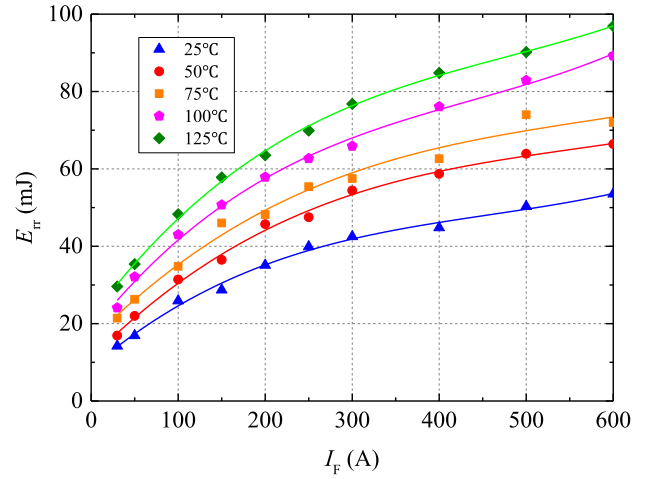


FIGURE 11. Recovery loss E_{rr} of the diode.

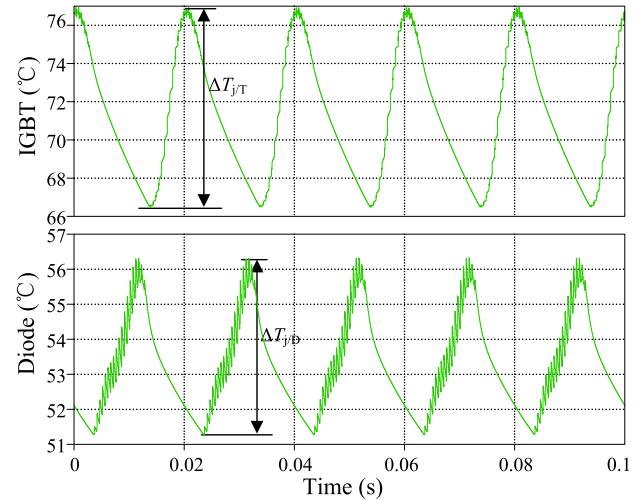


FIGURE 12. Thermal profiles of the power devices in PLECS.

TABLE 2. Comparison of the junction temperature fluctuations.

Power device	Current (RMS)	PLECS simulation	Proposed method	Two-step loss pulse method
IGBT	230A	10.3°C	10°C	14.1°C
Diode	230A	4.9°C	4.7°C	6.38°C

the steady-state junction temperature fluctuation is compared with the simulation results and the calculation results of the two-step pulse loss method, as shown in Table 2. Notably, compared with the simulation results, the accuracy of the proposed method is more satisfactory. It is worth noting that in the simulations the case temperatures of the IGBT and the diode are the same.

Table 2 shows the fundamental frequency fluctuations of the steady-state junction temperature of the IGBT and diode when the output current of the grid-side wind power converter is 230 A. In contrast, the calculated results based on the proposed method are very close to the simulation results of the PLECS steady-state junction temperature, and the errors are within 4%. However, the proposed method is faster and

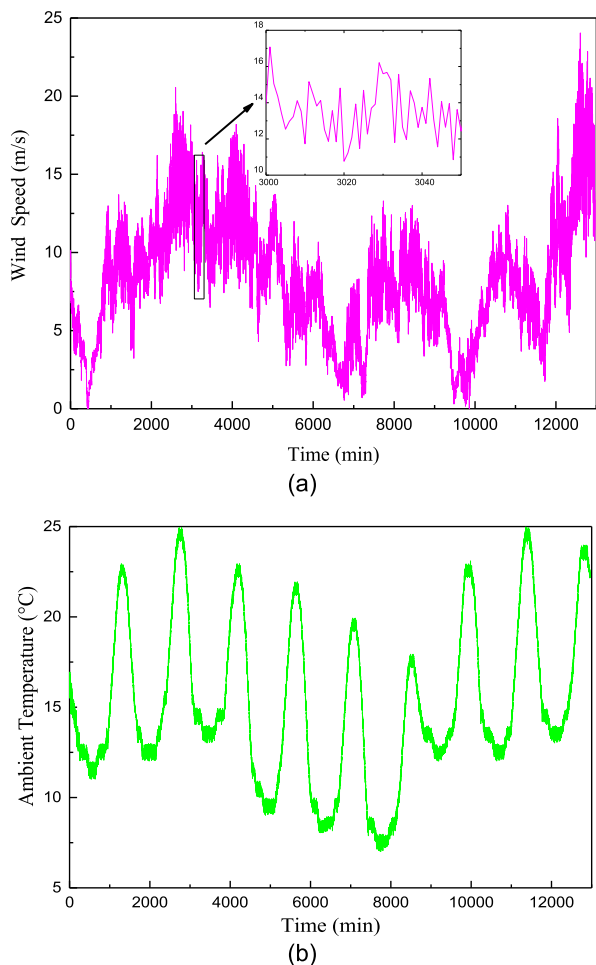


FIGURE 13. Data of the wind speed and ambient temperature. (a) Wind speed fluctuation curve. (b) Ambient temperature curve.

simpler. The maximum error based on the two-step pulse loss calculation is 37%. It can be seen that the method proposed in this paper has good accuracy when the output frequency is 50 Hz.

C. IMPACTS OF DIFFERENT OUTPUT FREQUENCIES

In the machine side of the converter and three-phase variable-frequency drive system, the output frequency is generally as low as 1 Hz, so it is necessary to study the sensitivity at low frequencies. To validate the calculation results, simulations are carried out using IPOSIM, where three-phase inverter models with different output frequencies are established. With the IPOSIM results as a reference, the results of the proposed method are compared with the results of the two-step loss pulse method. The same IGBT module is used as in the above experimental tests. For the case when the fundamental current of the inverter is 200 A, the results are shown in Table 3.

Table 3 shows the effect of the output fundamental frequency on the calculation method of the junction temperature fluctuation ΔT_j . Both the proposed method and the two-step pulse loss method are based on the same average

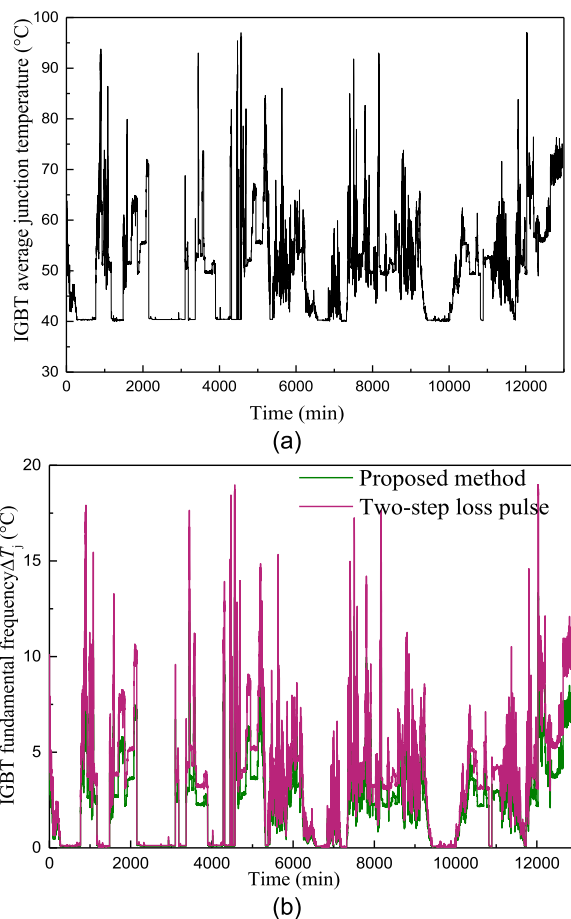


FIGURE 14. Average junction temperature and junction temperature fluctuation at the fundamental frequency. (a) Average junction temperature. (b) Junction temperature swing at the fundamental frequency.

losses of 269 W calculated by IPOSIM. For the same average power losses, the amplitude of the junction temperature fluctuation increases gradually with a decrease in the output frequency when using the same junction temperature calculation method. The calculation results of IPOSIM are used as a benchmark. When the output frequency is 50 Hz, the calculated results ΔT_j of the proposed method are consistent with those of the IPOSIM, while the error of the two-step pulse loss method is 41%. The calculated errors of the junction temperature fluctuations from 50 Hz to 5 Hz are less than the two-step pulse losses. However, when the output frequency is 1 Hz, the error of the two-step pulse loss method is 0.74%, while the error of the proposed method is 5.9%. The reason for this result is that the proposed junction temperature fluctuation calculation model assumes that the module needs to experience multiple sinusoidal half-wave losses before it can reach a stable state. However, when the module runs at a high temperature, it experiences one or several loss cycles, and the junction temperature can quickly reach a stable state. From Table 3, it can be seen that the proposed mathematical analysis method for the junction temperature fluctuation is applicable to different fundamental frequencies.

TABLE 3. Impacts of different output frequencies on the junction temperature fluctuation calculation based on the same IGBT power loss.

Fundamental frequency	Proposed method		IPOSIM calculation		Two-step loss pulse method	
	Average loss	ΔT_j	Average loss	ΔT_j	Average loss	ΔT_j
50 Hz	269 W	7.8°C	269 W	7.9°C	269 W	11.16°C
15 Hz	269 W	21.12°C	269 W	19.8°C	269 W	25.44°C
10 Hz	269 W	31.73°C	269 W	26.3°C	269 W	32.35°C
5 Hz	269 W	40.13°C	269 W	39.9°C	269 W	45.2°C
1 Hz	269 W	58.26°C	269 W	61.9°C	269 W	62.36°C

IV. FAST ESTIMATION OF THE JUNCTION TEMPERATURE WITH ACTUAL WIND SPEED DATA

Based on the high accuracy of the proposed junction temperature fluctuation model, the same IGBT module is used to quickly estimate the junction temperature of the grid-side converter. An SCADA system equipped with wind power grid-connected units can continuously store wind speed and cabin temperature data of wind turbines at a certain time interval. According to the mission profile, a reliability evaluation of the power devices can be carried out [30]. Consider the wind speed and temperature data collected by a wind farm in Hebei province for a period of time (12,960 min) as an example, as shown in Fig. 13. The data recording unit was 1 min, i.e., 12,960 wind conditions were recorded. Wind power converters use water-cooled heat dissipation, assuming that the temperature of the radiator is basically maintained at 40°C. When the wind speed is lower than the cut-in wind speed and the IGBT does not operate for more than 12 hours, the heat sink temperature is the internal temperature of the cabin. Based on the equivalent sinusoidal half-wave method, the average junction temperature and amplitude of the fundamental junction temperature fluctuation of the IGBT at each wind speed are obtained, which only takes approximately 3 s to improve the calculation speed significantly, as shown in Fig. 14. The two-step loss calculation is compared with the IGBT junction temperature fluctuation based on the equivalent sinusoidal half-wave loss calculation, as shown in Fig. 14(b). The green line represents the calculated value of the method proposed in this paper, and the magenta line represents the value of the two-step loss pulse calculation. Through the comparison, it can be seen that the two-step loss pulse method calculates a larger amplitude of the fundamental frequency junction temperature fluctuation. For the welded IGBT module, the cumulative life damage of the bonding line or chip solder layer will be overestimated when the latter calculation results are used to evaluate the life loss of the bonding line or chip solder layer. Therefore, the proposed method can predict the device life more accurately.

V. CONCLUSION

To estimation the lifetime of an IGBT module in wind power converters, it is necessary to address the junction temperature fluctuation at the fundamental frequency in the long-term mission profile quickly. Based on an equivalent sinusoidal half-wave loss, an analytical mathematical method is

proposed to estimate the fundamental junction temperature fluctuation more accurately in this paper. For actual wind speed data, a quantitative comparison is made with the two-step loss pulse method, which further validates the effectiveness of the proposed method.

A variation in the operational parameters is considered in the proposed method. The validity of the calculation of the junction temperature fluctuation is verified for output power frequencies through the grid-connected inverter model. Comparing the calculated results with the IPOSIM calculation and two-step loss pulse loss for different output frequencies, it is proved that the analytical model has high accuracy. In addition, the proposed method can also be applied to an IGBT module in a machine-side converter.

The calculated junction temperature fluctuations agree well with the time-domain simulation results. Compared with the two-step loss pulse method, the proposed calculation method for the junction temperature has high accuracy and achieves a fast calculation. Therefore, this method is suitable for calculating the cumulative damage device lifetimes over long time scales. In addition, the method is helpful for improving the accuracy of a reliability evaluation.

REFERENCES

- [1] F. Blaabjerg and K. Ma, "Future on power electronics for wind turbine systems," *IEEE J. Emerg. Sel. Topics Power Electron.*, vol. 1, no. 3, pp. 139–152, Sep. 2013.
- [2] C. Busca, R. Teodorescu, F. Blaabjerg, S. Munk-Nielsen, L. Helle, T. Abeyasekera, and P. Rodriguez, "An overview of the reliability prediction related aspects of high power IGBTs in wind power applications," *Microelectron. Rel.*, vol. 51, nos. 9–11, pp. 1903–1907, Sep./Nov. 2011.
- [3] L. Zeni, "Power oscillation damping from VSC–HVDC connected offshore wind power plants," *IEEE Trans. Power Del.*, vol. 31, no. 2, pp. 829–838, Apr. 2016.
- [4] R. Moeini, P. Tricoli, H. Hemida, and C. Baniotopoulos, "Increasing the reliability of wind turbines using condition monitoring of semiconductor devices: A review," *IET Renew. Power Gener.*, vol. 12, no. 2, pp. 182–189, Feb. 2018.
- [5] Y. Peng, L. Zhou, X. Du, P. Sun, K. Wang, and J. Cai, "Junction temperature estimation of IGBT module via a bond wires lift-off independent parameter V_{gE-np} ," *IET Power Electron.*, vol. 11, no. 2, pp. 320–328, Feb. 2018.
- [6] F. Spinato, P. J. Tavner, G. J. W. van Bussel, and E. Koutoulakos, "Reliability of wind turbine subassemblies," *IET Renew. Power Generat.*, vol. 3, no. 4, pp. 387–401, Dec. 2009.
- [7] S. Ariya, Y. Yongheng, S. Dezso, and B. Frede, "Lifetime evaluation of grid-connected PV inverters considering panel degradation rates and installation sites," *IEEE Trans. Power Electron.*, vol. 33, no. 2, pp. 1225–1236, Feb. 2018.
- [8] I. Vernica, H. Wang, and F. Blaabjerg, "Design for reliability and robustness tool platform for power electronic systems—Study case on motor drive applications," in *Proc. IEEE Appl. Power Electron. Conf. Expo. (APEC)*, Mar. 2018, pp. 1799–1806.

- [9] R. Burgos, G. Chen, F. Wang, D. Boroyevich, W. G. Odendaal, and J. D. Van Wyk, "Reliability-oriented design of three-phase power converters for aircraft applications," *IEEE Trans. Aerosp. Electron. Syst.*, vol. 48, no. 2, pp. 1249–1263, Apr. 2012.
- [10] M. Andresen, K. Ma, G. Buticchi, J. Falck, F. Blaabjerg, and M. Liserre, "Junction temperature control for more reliable power electronics," *IEEE Trans. Power Electron.*, vol. 33, no. 1, pp. 765–776, Jan. 2018.
- [11] U.-M. Choi, F. Blaabjerg, and S. Jørgensen, "Study on effect of junction temperature swing duration on lifetime of transfer molded power IGBT modules," *IEEE Trans. Power Electron.*, vol. 32, no. 8, pp. 6434–6443, Aug. 2017.
- [12] A. S. Bahman, K. Ma, and F. Blaabjerg, "A lumped thermal model including thermal coupling and thermal boundary conditions for high-power IGBT modules," *IEEE Trans. Power Electron.*, vol. 33, no. 3, pp. 2518–2530, Mar. 2018.
- [13] R. Tummala and E. Rymaszewski, *Microelectronics Packaging Handbook*. New York, NY, USA: Van Nostrand Reinold, 1989.
- [14] Y. Peng, "Study of IGBT junction temperature estimation based on turn-on miller platform voltage," (in Chinese), *Proc. CSEE*, vol. 37, no. 11, pp. 3254–3262 and 3381, Jun. 2017. doi: 10.13334/J.0258-8013.PCSEE.160972.
- [15] K. Xie, Z. Jiang, and W. Li, "Effect of wind speed on wind turbine power converter reliability," *IEEE Trans. Energy Convers.*, vol. 27, no. 1, pp. 96–104, Mar. 2012.
- [16] K. Ma, M. Liserre, F. Blaabjerg, and T. Kerekes, "Thermal loading and lifetime estimation for power device considering mission profiles in wind power converter," *IEEE Trans. Power Electron.*, vol. 30, no. 2, pp. 590–602, Feb. 2015.
- [17] X. Du, G. Li, J. Wu, P. Sun, and L. Zhou, "A junction temperature numerical calculation method for reliability evaluation in wind power converters," (in Chinese), *Proc. CSEE*, vol. 35, no. 11, pp. 2813–2821, Jun. 2015. doi: 10.13334/J.0258-8013.PCSEE.2015.11.020.
- [18] G. Li, X. Du, P. Sun, L. Zhou, and H. Tai, "Numerical IGBT junction temperature calculation method for lifetime estimation of power semiconductors in the wind power converters," in *Proc. Int. Power Electron. Appl. Conf. Expo.*, Shanghai, China, Nov. 2014, pp. 49–55.
- [19] I. R. Swan, A. T. Bryant, N.-A. Parker-Allotey, and P. A. Mawby, "3-D thermal simulation of power module packaging," in *Proc. IEEE Energy Convers. Congr. Expo.*, San Jose, CA, USA, Sep. 2009, pp. 1247–1254.
- [20] (2013). *Dimensioning Program IPOSIM for Loss and Thermal Calculation of Infineon IGBT Modules*. [Online]. Available: <https://infineon.transim.com/common>
- [21] K. Ma and F. Blaabjerg, "Reliability-cost models for the power switching devices of wind power converters," in *Proc. 3rd IEEE Int. Symp. Power Electron. Distrib. Gener. Syst. (PEDG)*, Aalborg, Denmark, Jun. 2012, pp. 820–827.
- [22] Y. Zhang, H. Wang, Z. Wang, Y. Yang, and F. Blaabjerg, "Simplified thermal modeling for IGBT modules with periodic power loss profiles in modular multilevel converters," *IEEE Trans. Ind. Electron.*, vol. 66, no. 3, pp. 2323–2332, Mar. 2019.
- [23] A. Patel, S. Joshi, H. Chandwani, V. Patel, and K. Patel, "Estimation of junction temperature and power loss of an IGBT used in VVVF inverter using numerical solution from data sheet parameter," in *Proc. Int. J. Comput. Commun. Inf. Syst.*, vol. 2, Jul./Dec. 2010, pp. 17–22.
- [24] K. Ma, M. Liserre, and F. Blaabjerg, "Operating and loading conditions of a three-level neutral-point-clamped wind power converter under various grid faults," *IEEE Trans. Ind. Appl.*, vol. 50, no. 1, pp. 520–530, Jan./Feb. 2014.
- [25] A. A. Hadi, X. Fu, and R. Challoor, "IGBT module loss calculation and thermal resistance estimation for a grid-connected multilevel converter," *Proc. SPIE*, vol. 10754, Sep. 2018, Art. no. 107540F.
- [26] A. Isidori, F. M. Rossi, F. Blaabjerg, and K. Ma, "Thermal loading and reliability of 10-MW multilevel wind power converter at different wind roughness classes," *IEEE Trans. Ind. Appl.*, vol. 50, no. 1, pp. 484–494, Jan./Feb. 2013.
- [27] P. Ganesan, R. Manju, K. R. Razila, and J. V. Rinu, "Characterisation of 1200V, 35A SiC Mosfet using double pulse circuit," in *Proc. IEEE Int. Conf. Power Electron., Drives Energy Syst. (PEDES)*, Dec. 2016, pp. 1–6.
- [28] J. Schönberger, "Averaging methods for electrical-thermal converter models," in *Proc. 14th Eur. Conf. Power Electron. Appl.*, Aug./Sep. 2011, pp. 1–8.

- [29] H. Huang and P. A. Mawby, "A lifetime estimation technique for voltage source inverters," *IEEE Trans. Power Electron.*, vol. 28, no. 8, pp. 4113–4119, Aug. 2013.
- [30] Y. Zhang, H. Wang, Z. Wang, Y. Yang, and F. Blaabjerg, "The impact of mission profile models on the predicted lifetime of IGBT modules in the modular multilevel converter," in *Proc. 43rd Annu. Conf. IEEE Ind. Electron. Soc.*, Beijing, China, Oct./Nov. 2017, pp. 7980–7985.



XIPING WANG was born in Hebei, China. She received the B.S. and M.S. degrees in electrical engineering from Shenyang Agriculture University, Shenyang, China, in 2003 and 2006, respectively. She is currently pursuing the Ph.D. degree with the State Key Laboratory of Reliability and Intelligence of Electrical Equipment, School of Electrical Engineering, Hebei University of Technology, Tianjin, China.

Her current research interests include the reliability of power electronics, including the physics-of-failure analysis of reliability critical components and design for reliability methods for power electronic applications and multilevel converters.



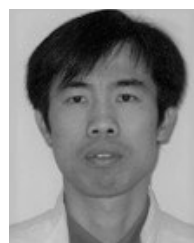
ZHIGANG LI received the Ph.D. degree in electrical engineering from the Hebei University of Technology, Tianjin, China, in 1998.

Since 1996, he has been a Professor with the School of Electrical Engineering, Hebei University of Technology, where he is currently a Researcher with the State Key Laboratory of Reliability and Intelligence of Electrical Equipment. His current research interests include wind power generation, electrical reliability and testing technology, and electrical and electronic research work.



FANG YAO was born in Tianjin, China. She received the B.S. degree in electronics and information system from Jilin University, Changchun, China, in 1995, and the M.S. and Ph.D. degrees in electric machines and electric apparatus from the Hebei University of Technology, Tianjin, in 2001 and 2004, respectively, where she is currently a Full Professor with the State Key Laboratory of Reliability and Intelligence of Electrical Equipment. Her current research interests include

the reliability research on device and equipment in electrical engineering and microgrid techniques.



SHENGXUE TANG received the M.S. and Ph.D. degrees in electrical engineering from Hunan University, Changsha, China, in 2004 and 2008, respectively.

From 2009 to 2016, he was a Visiting Professor with the College of Electrical Engineering, Hebei University of Technology, Tianjin, China, where he was a Professor with the College of Electrical Engineering, from 2016 to 2019. He is the author of more than 30 articles. His current research interests include signal processing in electrical engineering, power devices reliability, and microgrids and converter techniques.